

Atomic Radii for Depicting Atoms in a Molecule II: The Effective Atomic Radius and van der Waals Radius from $_1$H to $_{54}$Xe

Hiroshi Tatewaki,*[1,2] Yasuyo Hatano,[3] Takatoshi Naka,[3] Takeshi Noro,[4] and Shigeyoshi Yamamoto[5]

[1]Graduate School of Natural Sciences, Nagoya City University, Nagoya 467-8501

[2]Institute of Advanced Studies in Artificial Intelligence, Chukyo University, Toyota 470-0393

[3]School of Information Science and Technology, Chukyo University, Toyota 470-0393

[4]Division of Chemistry, Graduate School of Science, Hokkaido University, Sapporo 060-0810

[5]School of International Liberal Studies, Chukyo University, Nagoya 466-8666

Received June 17, 2010; E-mail: htatewak@nsc.nagoya-cu.ac.jp

We consider the effective atomic radius (r_{ear}), defined as the distance from the nucleus at which the magnitude of the electric field is that in He at one half of the equilibrium bond length of He_2, for atoms from H to Xe. The value of r_{ear} accurately reflects the electronic configuration; for example, the effective radius shortens smoothly from B $2s^22p^1$ to Ne $2s^22p^6$, in contrast to the van der Waals radius (r_{vdW}) which behaves irregularly with atomic number from B to Ne. The valence radii (r_{val}) are also defined and discussed. Values of r_{ear} and r_{val} are used to depict the electron charge distribution of the homonuclear diatomic molecules of groups 15, 18, and transition-metal atoms, and provide insight into the characteristics of these molecules.

To characterize the appropriate atomic size (radius) for imaging the charge distribution when atoms are placed at the equilibrium positions in chemical substances, we recently defined the effective atomic radius (r_{ear}),[1] which is the distance from the nucleus at which the magnitude of the electric field (E) is the same as that in He at one half of the equilibrium bond length of He_2; $r_{ear} = r$ at which $E = E_{He}$ ($r = R_e/2$ of He_2). In the previous paper we gave the values of r_{ear} for He, Ne, Ar, Kr, Xe, and Cu.

Apart from the radius r_{ear}, three types of radius of an atom can be specified, as follows:

1) The radius at which the atom begins to interact with other atoms, which is known as the van der Waals radius (r_{vdW}).[2]

2) The radius corresponding to the valence region, including the maximum of the valence charge distribution and a large proportion (around 60%) of the valence electrons, which will be called the valence radius (r_{val}).[3,4]

3) The radius inside which the electrons of the other atoms scarcely encroach, which will be called the core radius (r_{core}).[1]

The radii r_{vdW} and r_{val} are based on models that construct crystals out of spheres, and in which the bonding atoms approximately touch. The characteristics of the crystals constrain the characteristics of the radii. Analogous to the valence radius, Yang and Davidson[5] specified a boundary radius which is obtained by requiring an approximate potential to be equal to the ionization potential. Before our previous study,[1] we believed that the van der Waals radius (r_{vdW}) was adequate to describe the size of the atom as revised by Bondi[6] and recently by Mantina and co-workers[7] who used ab initio CI calculations with and without relativistic effects approximated by the Douglas–Kroll–Hess (DK) transformation.[8,9] It is shown below that the vdW-radius of some atoms given by Bondi is not an adequate measure of their atomic size.

For elements in groups 1, 2, 10, 11, and 12, the r_{vdW} is smaller than or approximately equal to the mean value r ($\langle r \rangle$) of the outermost shell, so that the vdW-radius specified above is inappropriate to characterize the atomic size. For example, the r_{vdW} values for $_3$Li and $_{37}$Rb are 1.81 and 3.03 Å respectively, whereas $\langle r \rangle_{2s} = 2.05$ Å for Li and $\langle r \rangle_{5s} = 2.94$ Å for Rb; also r_{vdW} for $_{29}$Cu and $_{47}$Ag are 1.40 and 1.72 Å respectively, but $\langle r \rangle_{4s} = 1.73$ Å for Cu and $\langle r \rangle_{5s} = 1.83$ Å for Ag (Tables 1 and 4, set out in the next section). The r_{vdW} values are too small as a measure of the radii at which the atoms begin to interact with each other. These discrepancies arise because of the use of data from the bulk solid state. To our surprise, we also found that r_{vdW} increases between group 17 and 18. On the other hand, the r_{ear} value for $_{29}$Cu was 2.93 Å, which is considerably greater than $\langle r \rangle_{4s} = 1.73$ Å, indicating that r_{ear} might be the atomic radius at which interatomic interaction begins. From the definition of r_{ear} we expect that it directly reflects the atomic electronic structure, and decreases smoothly with increasing atomic number of the elements of the group. In the present work we look at the atomic radius r_{ear}, for atoms H to Xe, which gives the same magnitude of electric field as E_{He} ($r = R_e/2$ of He_2).

We shall also determine the valence radius (r_{val}). For r_{val} we adopted the mean value of r, denoted $\langle r \rangle$, as suggested by Slater.[3] The second section sets out the method of calculation. The third section gives the effective atomic radii and valence radii for $_1$H to $_{54}$Xe, calculated with relativistic effects given by the Douglas–Kroll–Hess transformation.[8,9] The fourth section presents electron densities for selected diatomic molecules,

Published on the web October 5, 2010; doi:10.1246/bcsj.20100166

imaged using the effective atomic radii (r_{ear}). A summary is given in the last section.

Theoretical Methods

He_2 is a typical vdW-molecule, and has the smallest dissociation energy (D_e) of the diatomics. As in the previous work,[1] we define r_{ear} as the radius at which the electric field is equal in magnitude to E_{He} ($r = R_e/2$ of He_2). The expectation value of the electric field is calculated using the program GAMESS.[10] It was shown in the earlier paper[1] that finding the r value of the atom I giving the same electric field as E_{He} ($r = R_e/2$ of He_2) is approximately equivalent to finding r for the atom I giving the same charge density as $|F_{He}$ ($r = R_e/2$ of $He_2)|^2$, where $|F(r)|^2$ is the radial density at r. Nonrelativistic Hartree–Fock (NR-HF) wave functions, nonrelativistic configuration interaction singles and doubles (NR-CISD) wave functions, relativistic HF with third-order DK Hamiltonian (DK-HF) wave functions[11] and relativistic CISD (DK-CISD) wave functions all gave virtually identical r_{ear} values for the inert gas atoms except for Xe. In the case of Xe, the differences between the nonrelativistic and relativistic calculations are obvious, although small (0.02 Å); the smaller DK values of r_{ear} for Xe than the NR values stem from relativistic corrections, which effectively increase the nuclear charge, resulting in a contraction of the charge distribution (atomic size). For convenience and generality, we adopt DK-HF. The basis sets used for the respective calculations are the contracted Gaussian-type functions (GTFs),[12] and are divided into: H–He (5111), Li–Be (7211), B–Ne (7211/4111), Na–Mg (7421/7), Al–Ar (7421/7211), K–Ca (84321/74), Sc–Zn (84321/74/4111), Ga–Kr (84321/7421/7), Rb–Sr (843321/743/7), Y–Cd (843321/743/7211), and In–Xe (843321/74321/74).

In the previous paper we defined the valence radius as

$$\langle r\rangle = \left\{\sum_i n_{is}(is|r|is) + \sum_i n_{ip}(ip|r|ip)\right\} \Big/ \left(\sum_i n_{is} + \sum_i n_{ip}\right) \quad (1)$$

In general, atomic valence orbitals have different principal quantum numbers. We therefore use the valence radius defined by

$$\langle r\rangle_{nl} = \langle nl|r|nl\rangle \quad (2)$$

where n and l are the principal and angular-momentum quantum numbers of the valence atomic orbital. It will be shown that 52%–60% of the nl valence electrons are within the sphere defined by $\langle r\rangle_{nl}$.

Results

To obtain the values of r_{ear}, we first calculated E_{He} ($r = R_e/2$ of He_2). Its value is 0.00226 au. We, here, do not consider the picture change effect/error (PCE)[13–16] for the Douglas–Kroll–Hess relativistic calculations. The PCE is significant for the physical quantities which have large values in the vicinity of the nucleus.[13–16] Therefore, the PCE is expected to be small, since the electric field far from the nucleus is treated in the present work.

Li to Be, B to Ne. In Table 1, the values of $\langle r\rangle_{ns}$, $\langle r\rangle_{np}$, r_{ear}, and r_{Bondi} are set out for typical elements; we list r_{Bondi}, which is modified via modern quantum chemistry calculations.[7]

Table 1. Mean Distance r ($\langle r\rangle_{nl}$), Effective Atomic Radius (r_{ear}), and Bondi's Radius (r_{Bondi}) for Typical Elements from $_1$H to $_{54}$Xe (in Å)

	$_1$H							$_2$He
$\langle r\rangle_{1s}$	0.79							0.49
r_{ear}	1.87							1.49
r_{Bondi}	1.10							1.40
	$_3$Li	$_4$Be	$_5$B	$_6$C	$_7$N	$_8$O	$_9$F	$_{10}$Ne
$\langle r\rangle_{2s}$	2.05	1.40	1.05	0.84	0.70	0.60	0.53	0.47
$\langle r\rangle_{2p}$			1.17	0.91	0.75	0.65	0.57	0.51
r_{ear}	3.30	2.79	2.51	2.24	2.02	1.91	1.79	1.68
r_{Bondi}	1.81	1.53	1.92	1.70	1.55	1.52	1.47	1.54
	$_{11}$Na	$_{12}$Mg	$_{13}$Al	$_{14}$Si	$_{15}$P	$_{16}$S	$_{17}$Cl	$_{18}$Ar
$\langle r\rangle_{3s}$	2.23	1.72	1.37	1.16	1.02	0.91	0.82	0.75
$\langle r\rangle_{3p}$			1.82	1.46	1.23	1.09	0.97	0.88
r_{ear}	3.46	3.16	3.14	2.87	2.63	2.50	2.35	2.21
r_{Bondi}	2.27	1.73	1.84	2.10	1.80	1.80	1.75	1.88
	$_{19}$K	$_{20}$Ca	$_{31}$Ga	$_{32}$Ge	$_{33}$As	$_{34}$Se	$_{35}$Br	$_{36}$Kr
$\langle r\rangle_{4s}$	2.77	2.22	1.30	1.16	1.06	0.97	0.90	0.85
$\langle r\rangle_{4p}$			1.81	1.51	1.33	1.21	1.11	1.03
r_{ear}	3.97	3.73	3.10	2.92	2.74	2.65	2.53	2.41
r_{Bondi}	2.75	2.31	1.87	2.11	1.85	1.90	1.83	2.02
	$_{37}$Rb	$_{38}$Sr	$_{49}$In	$_{50}$Sn	$_{51}$Sb	$_{52}$Te	$_{53}$I	$_{54}$Xe
$\langle r\rangle_{5s}$	2.94	2.42	1.44	1.31	1.22	1.13	1.07	1.01
$\langle r\rangle_{5p}$			1.99	1.71	1.52	1.41	1.31	1.22
r_{ear}	4.12	3.93	3.28	3.13	2.96	2.89	2.78	2.67
r_{Bondi}	3.03	2.49	1.93	2.17	2.06	2.06	1.98	2.16

Table 2. Number of nl Valence Electrons (NVEs) and NVE in Spheres Having Radius $\langle r\rangle_{nl}$ and r_{ear} of Typical Atoms

	$_1$H							$_2$He
$\langle r\rangle_{1s}$	0.58							1.17
r_{ear}	0.97							1.98
	$_3$Li	$_4$Be	$_5$B	$_6$C	$_7$N	$_8$O	$_9$F	$_{10}$Ne
$\langle r\rangle_{2s}$	0.56	1.13	1.14	1.14	1.14	1.14	1.14	1.14
$\langle r\rangle_{2p}$			0.57	1.16	1.74	2.34	2.94	3.53
r_{ear}	0.91	1.94	2.95	3.96	4.97	5.97	6.97	7.98
	$_{11}$Na	$_{12}$Mg	$_{13}$Al	$_{14}$Si	$_{15}$P	$_{16}$S	$_{17}$Cl	$_{18}$Ar
$\langle r\rangle_{3s}$	0.56	1.13	1.13	1.12	1.12	1.12	1.12	1.11
$\langle r\rangle_{3p}$			0.57	1.13	1.70	2.28	2.85	3.42
r_{ear}	0.90	1.92	2.92	3.93	4.94	5.95	6.96	7.96
	$_{19}$K	$_{20}$Ca	$_{31}$Ga	$_{32}$Ge	$_{33}$As	$_{34}$Se	$_{35}$Br	$_{36}$Kr
$\langle r\rangle_{4s}$	0.56	1.12	1.13	1.13	1.12	1.12	1.11	1.11
$\langle r\rangle_{4p}$			0.57	1.14	1.70	2.28	2.85	3.41
r_{ear}	0.87	1.89	2.92	3.93	4.94	5.94	6.95	7.95
	$_{37}$Rb	$_{38}$Sr	$_{49}$In	$_{50}$Sn	$_{51}$Sb	$_{52}$Te	$_{53}$I	$_{54}$Xe
$\langle r\rangle_{5s}$	0.56	1.12	1.12	1.12	1.11	1.11	1.10	1.10
$\langle r\rangle_{5p}$			0.57	1.13	1.69	2.26	2.82	3.37
r_{ear}	0.86	1.87	2.91	3.92	4.93	5.93	6.94	7.94

Table 2 sets out the numbers of the nl valence electrons (nl NVE) in the sphere defined by $\langle r\rangle_{nl}$ and r_{ear}. Table 3 gives the ratio of nl NVE in the sphere having radius $\langle r\rangle_{nl}$ to nl NVE, and the ratio of the total NVE in the sphere defined by r_{ear} to the total NVE. Figure 1 shows r_{ear}, r_{Bondi}, and r_{val}, where r_{val} is the greatest $\langle r\rangle$ among the values of $\langle r\rangle_{nl}$ for the respective atoms.

Table 3. Ratio of *nl* NVE within Sphere of Radius $\langle r\rangle_{nl}$ to *nl* NVE, and Ratio of NVE in Sphere with r_{ear} to NVE for Typical Atoms

	$_1$H							$_2$He
$\langle r\rangle_{1s}$	0.58							0.59
r_{ear}	0.97							0.99
	$_3$Li	$_4$Be	$_5$B	$_6$C	$_7$N	$_8$O	$_9$F	$_{10}$Ne
$\langle r\rangle_{2s}$	0.56	0.57	0.57	0.57	0.57	0.57	0.57	0.57
$\langle r\rangle_{2p}$			0.57	0.58	0.58	0.58	0.59	0.59
r_{ear}	0.91	0.97	0.98	0.99	0.99	1.00	1.00	1.00
	$_{11}$Na	$_{12}$Mg	$_{13}$Al	$_{14}$Si	$_{15}$P	$_{16}$S	$_{17}$Cl	$_{18}$Ar
$\langle r\rangle_{3s}$	0.56	0.57	0.56	0.56	0.56	0.56	0.56	0.56
$\langle r\rangle_{3p}$			0.57	0.57	0.57	0.57	0.57	0.57
r_{ear}	0.90	0.96	0.97	0.98	0.99	0.99	0.99	1.00
	$_{19}$K	$_{20}$Ca	$_{31}$Ga	$_{32}$Ge	$_{33}$As	$_{34}$Se	$_{35}$Br	$_{36}$Kr
$\langle r\rangle_{4s}$	0.56	0.56	0.57	0.56	0.56	0.56	0.56	0.55
$\langle r\rangle_{4p}$			0.57	0.57	0.57	0.57	0.57	0.57
r_{ear}	0.87	0.95	0.97	0.98	0.99	0.99	0.99	0.99
	$_{37}$Rb	$_{38}$Sr	$_{49}$In	$_{50}$Sn	$_{51}$Sb	$_{52}$Te	$_{53}$I	$_{54}$Xe
$\langle r\rangle_{5s}$	0.56	0.56	0.56	0.56	0.56	0.55	0.55	0.55
$\langle r\rangle_{5p}$			0.57	0.57	0.56	0.56	0.56	0.56
r_{ear}	0.86	0.94	0.97	0.98	0.99	0.99	0.99	0.99

The values of r_{Bondi} for $_3$Li and $_4$Be are less than or nearly equal to $\langle r\rangle_{2s}$, indicating the inadequacy of r_{Bondi} as a van der Waals radius at which the atoms begins to make contact with others; the sphere specified by $\langle r\rangle_{2s}$ includes only 56%–57% of the valence 2s electrons (Table 3). In contrast, the values of r_{ear} for Li and Be are 3.30 and 2.79 Å (Table 1), which are 1.6–2.0 times greater than $\langle r\rangle_{2s}$. The values of r_{ear} are candidates for the radius at which the interatomic interaction begins; the sphere specified by r_{ear} includes 91%–97% of the valence 2s electrons. As also shown in Figure 1, r_{ear} decreases monotonically from B to Ne, whereas r_{Bondi} is minimum for F and increases toward Ne; according to Table 3, the sphere specified by r_{ear} includes 98%–≈100% of the valence electrons. The trend of r_{Bondi} is surprising, since the atomic size is expected to decrease as the atomic number increases up to the electron configuration $2s^22p^n$; the decrease in the atomic size stems from incompleteness of the shielding effect of a valence electron. In fact, from H to He, the r_{Bondi} increases whereas the r_{ear} decreases.

Na to Mg, Al to Ar. The values of r_{Bondi} for $_{11}$Na and $_{12}$Mg are less than or nearly equal to the respective $\langle r\rangle_{3s}$ values as the r_{Bondi}s as for Li and Be, which shows the inadequacy of r_{Bondi} as a *van der Waals radius* at which the mutual interaction begins. In contrast, the values of r_{ear} for Na and Mg are 3.46 and 3.16 Å, which are 1.6–1.8 times greater than $\langle r\rangle_{3s}$, showing that r_{ear} is adequate as a *van der Waals radius*. Figure 1 and Table 1 indicate that r_{ear} decreases monotonically from $_{13}$Al to $_{18}$Ar, whereas r_{Bondi} is greatest at $_{14}$Si not at Al, is equal for $_{15}$P and $_{16}$S, is least for $_{17}$Cl, and increases toward $_{18}$Ar. This trend for r_{Bondi} contradicts our expectation. We see from Table 3 that the sphere given by r_{ear} includes 97%–≈100% of the valence electrons.

K to Ca, Ga to Kr, and Rb to Sr, In to Xe. The behavior of r_{ear} and r_{Bondi} for the elements in groups 1 and 2 ($_{19}$K and $_{20}$Ca, $_{37}$Rb and $_{38}$Sr) versus atomic number parallels that of Na and Mg. Also, behaviors for the elements of the groups 13–18 $_{31}$Ga to $_{36}$Kr and $_{49}$In to $_{54}$Xe, parallel those for B to Ne and Al to Ar. It is found that r_{Bondi} is smaller that or near to $\langle r\rangle_{ns}$ in group 1 and group 2, and is greatest at group 14 ($_{32}$Ge/$_{50}$Sn) not group 13 ($_{31}$Ga/$_{49}$In). The two measures (r_{Bondi}s) are nearly equal in groups 15 ($_{33}$As/$_{51}$Sb) and 16 ($_{34}$Se/$_{52}$T2), and it is smallest at group 17 ($_{35}$Br/$_{53}$I), with a small increase to group 18. In contrast, r_{ear} decreases monotonically from group 13 to group 18. The NVEs within the r_{ear} sphere decrease gradually in number down the periodic table.

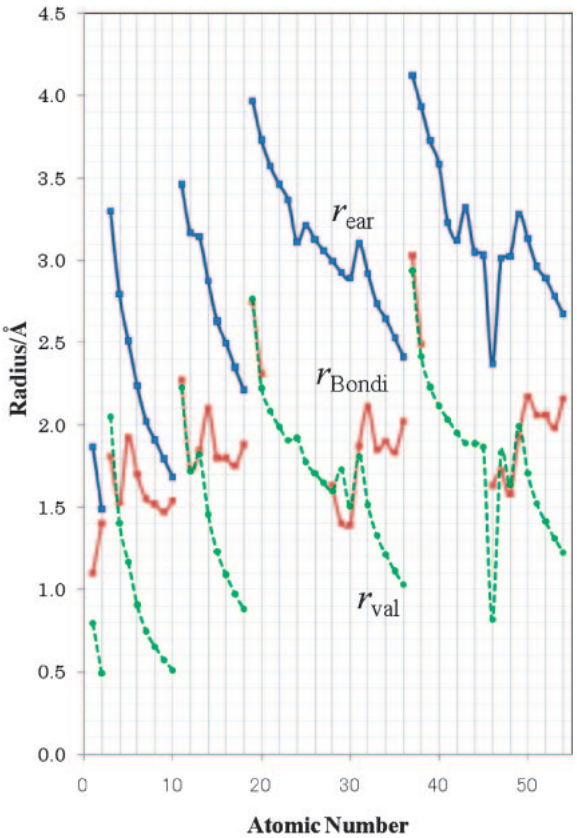

Figure 1. The radii r_{ear} in blue, r_{Bondi} in red, and r_{val} in green for H through Xe (Å).

Sc to Zn. In Table 4, $\langle r\rangle_{ns}$, $\langle r\rangle_{(n-1)d}$, $\langle r\rangle_{(n-1)p}$, $\langle r\rangle_{(n-1)s}$, r_{ear}, and r_{Bondi} are set out for the first and second transition metal atoms; r_{Bondi} is given for the elements in groups 10–12.[6] In Table 5, the number of *nl* valence electrons (NVEs) in the spheres defined by $\langle r\rangle_{ns}$ and $\langle r\rangle_{(n-1)l}$ is set out, together with NVE in the r_{ear} sphere. Table 6 gives the ratio of *nl* NVE in the sphere defined by $\langle r\rangle_{nl}$ to *nl* NVE, and also the ratio of the NVE in the r_{ear} sphere to the (total) NVE. Values of r_{ear}, r_{Bondi}, and r_{val} have already been given in Figure 1.

Table 4 and Figure 1 show that r_{ear} decreases monotonically with increasing atomic number except for $_{24}$Cr, which has the electron configuration $4s^13d^5$, distinct from $4s^23d^n$ of the others, excluding Cu which has $4s^13d^{10}$. As discussed in the next subsection below **Y to Cd**, the r_{ear} depends on the charge distribution defined by the ground state electron configuration. One may then claim that why r_{ear} does not sharply decrease at Cu which has $4s^13d^{10}$. It is seen in Table 4 that the decrement in r_{ear} between Ni and Cu is greater than that between Cu and Zn, indicating that r_{ear} according to $4s^13d^{10}$ is smaller than that

Table 4. Mean Distance r ($\langle r\rangle_{nl}$), Effective Atomic Radius (r_{ear}), and Bondi's Radius (r_{Bondi}) for the First and Second Transition Metal Atoms (in Å)

	$_{21}$Sc	$_{22}$Ti	$_{23}$V	$_{24}$Cr	$_{25}$Mn	$_{26}$Fe	$_{27}$Co	$_{28}$Ni	$_{29}$Cu	$_{30}$Zn
$\langle r\rangle_{4s}$	2.08	1.99	1.91	1.92	1.77	1.71	1.65	1.60	1.73	1.51
$\langle r\rangle_{3d}$	0.89	0.78	0.70	0.73	0.60	0.57	0.54	0.51	0.53	0.47
$\langle r\rangle_{3p}$	0.62	0.58	0.54	0.52	0.48	0.46	0.43	0.41	0.40	0.38
$\langle r\rangle_{3s}$	0.57	0.53	0.50	0.48	0.45	0.43	0.41	0.39	0.38	0.36
r_{ear}	3.57	3.46	3.37	3.11	3.21	3.13	3.06	3.00	2.93	2.89
r_{Bondi}								1.63	1.40	1.39
	$_{39}$Y	$_{40}$Zr	$_{41}$Nb	$_{42}$Mo	$_{43}$Tc	$_{44}$Ru	$_{45}$Rh	$_{46}$Pd	$_{47}$Ag	$_{48}$Cd
$\langle r\rangle_{5s}$	2.23	2.12	2.03	1.95	1.89	1.89	1.86		1.83	1.64
$\langle r\rangle_{4d}$	1.32	1.13	1.11	1.01	0.87	0.87	0.82	0.82	0.73	0.67
$\langle r\rangle_{4p}$	0.77	0.73	0.69	0.66	0.63	0.60	0.58	0.56	0.53	0.51
$\langle r\rangle_{4s}$	0.68	0.65	0.62	0.59	0.56	0.54	0.52	0.51	0.49	0.47
r_{ear}	3.73	3.58	3.23	3.12	3.32	3.05	3.03	2.37	3.01	3.02
r_{Bondi}								1.63	1.72	1.58

Table 6. Ratio of *nl* NVE within Sphere of Radius $\langle r\rangle_{nl}$ to *nl* NVE, and Ratio of NVE in Sphere with r_{ear} to NVE for Transition-Metal Atoms

	$_{21}$Sc	$_{22}$Ti	$_{23}$V	$_{24}$Cr	$_{25}$Mn	$_{26}$Fe	$_{27}$Co	$_{28}$Ni	$_{29}$Cu	$_{30}$Zn
$\langle r\rangle_{4s}$	0.56	0.56	0.56	0.56	0.57	0.57	0.57	0.57	0.57	0.57
$\langle r\rangle_{3d}$	0.59	0.59	0.59	0.60	0.59	0.59	0.59	0.60	0.61	0.60
$\langle r\rangle_{3p}$	0.56	0.56	0.56	0.56	0.56	0.55	0.57	0.55	0.56	0.55
$\langle r\rangle_{3s}$	0.55	0.54	0.54	0.55	0.54	0.54	0.54	0.54	0.55	0.54
r_{ear}	0.99	0.99	0.99	0.99	0.99	1.00	1.00	1.00	1.00	1.00
	$_{39}$Y	$_{40}$Zr	$_{41}$Nb	$_{42}$Mo	$_{43}$Tc	$_{44}$Ru	$_{45}$Rh	$_{46}$Pd	$_{47}$Ag	$_{48}$Cd
$\langle r\rangle_{5s}$	0.56	0.56	0.56	0.56	0.56	0.56	0.56		0.57	0.57
$\langle r\rangle_{4d}$	0.58	0.58	0.58	0.58	0.57	0.58	0.58	0.59	0.58	0.58
$\langle r\rangle_{4p}$	0.55	0.55	0.55	0.55	0.55	0.55	0.55	0.55	0.54	0.54
$\langle r\rangle_{4s}$	0.54	0.54	0.54	0.54	0.53	0.53	0.53	0.52	0.53	0.53
r_{ear}	0.99	0.99	0.99	0.99	0.99	1.00	1.00	1.00	1.00	1.00

Table 5. Number of *nl* Valence Electrons (NVEs) and NVE within Spheres of Radius $\langle r\rangle_{nl}$ and r_{ear} for Transition-Metal Atoms

	$_{21}$Sc	$_{22}$Ti	$_{23}$V	$_{24}$Cr	$_{25}$Mn	$_{26}$Fe	$_{27}$Co	$_{28}$Ni	$_{29}$Cu	$_{30}$Zn
$\langle r\rangle_{4s}$	1.12	1.12	1.13	0.56	1.13	1.13	1.13	1.14	0.57	1.14
$\langle r\rangle_{3d}$	0.59	1.18	1.76	3.00	2.95	3.56	4.16	4.77	6.08	5.98
$\langle r\rangle_{3p}$	3.33	3.33	3.33	3.35	3.33	3.33	3.40	3.33	3.34	3.33
$\langle r\rangle_{3s}$	1.09	1.09	1.09	1.09	1.09	1.09	1.09	1.09	1.09	1.09
r_{ear}	10.90	11.90	12.91	13.92	14.92	15.92	16.92	17.93	18.93	19.93
	$_{39}$Y	$_{40}$Zr	$_{41}$Nb	$_{42}$Mo	$_{43}$Tc	$_{44}$Ru	$_{45}$Rh	$_{46}$Pd	$_{47}$Ag	$_{48}$Cd
$\langle r\rangle_{5s}$	1.12	1.12	0.56	0.56	1.13	0.56	0.56		0.57	1.13
$\langle r\rangle_{4d}$	0.58	1.16	2.34	2.92	2.87	4.09	4.68	5.94	5.83	5.76
$\langle r\rangle_{4p}$	3.31	3.29	3.30	3.29	3.27	3.28	3.27	3.28	3.26	3.25
$\langle r\rangle_{4s}$	1.08	1.08	1.08	1.07	1.07	1.07	1.07	1.05	1.07	1.06
r_{ear}	10.89	11.90	12.92	13.92	14.91	15.92	16.93	17.95	18.93	19.93

according to $4s^23d^9$. The values of r_{Bondi} listed are less than or equal to the corresponding $\langle r\rangle_{4s}$, and the sphere defined by $\langle r\rangle_{4s}$ contains 57% of the electrons in the 4s orbital (Table 6). Again, the experimental van der Waals radius or the r_{Bondi} as a measure of an atomic size is doubtful.

Y to Cd. Three kinds of electron configuration are recognized for the second transition metal atoms: $5s^24d^n$ for $_{39}$Y, $_{40}$Zr, $_{43}$Tc, $_{48}$Cd; $5s^14d^{n+1}$ for $_{41}$Nb, $_{42}$Mo, $_{44}$Ru, $_{45}$Rh, $_{47}$Ag; and $5s^04d^{n+2}$ for $_{46}$Pd. We therefore distinguish three kinds of r_{ear}: $r_{ear}(5s^24d^n)$, $r_{ear}(5s^14d^{n+1})$, and $r_{ear}(5s^04d^{n+2})$. Our previous paper disclosed that to find the r value of the atom I giving the same electric field as E_{He} ($r = R_e/2$ of He_2) is approximately equivalent to finding r for the atom I giving the same charge density as $|F_{He}$ (r at $R_e/2$ of $He_2)|^2$, where $|F|^2$ is the radial density. The $5s^24d^n$ configuration has the most diffuse charge distribution, with $5s^14d^{n+1}$, next, and $5s^04d^{n+2}$ the smallest, if compared in the same atom. Upon calculating $r_{ear}(5s^24d^n)$, $r_{ear}(5s^14d^{n+1})$, and $r_{ear}(5s^04d^{n+2})$ for all atoms from Y to Cd, we can draw three graphs of r_{ear}: the largest for $5s^24d^n$, the next for $5s^14d^{n+1}$, and the smallest for $5s^04d^{n+2}$. The r_{ear} selects one of the three, following the optimum atomic electron configuration. The number of electrons in the sphere of radius r_{ear} contains 99%–≈100% of the total valence (5s, 4d, 4p, 4s) electrons, while the sphere of radius $\langle r\rangle_{nl}$ contains 52%–59% of the corresponding *nl* electrons (Table 6). The value of r_{Bondi} for Ag and Cd is smaller than $\langle r\rangle_{5s}$; use of the experimental van der Waals radius or r_{Bondi} as a measure of atomic size is again questionable.

Application

Consider now the electron charge density of the homonuclear diatomic molecules. We put one of the two atoms at (0, 0, $-R_e/2$) and the other at (0, 0, $R_e/2$), where R_e is an equilibrium internuclear distance (Å) determined by experiment. With the two atoms as centers, we consider the sphere given by r_{ear} and the surface of density $|F(x,y,z)_{nl}|^2$ for the *nl* atomic orbital which contains *nl* electrons given in Table 2 or Table 5. The experimental dissociation energy (D_e) and the equilibrium internuclear distance (R_e) are also used to discuss the characteristics of the molecule.

Group 15 Diatoms (N_2, P_2, As_2, and Sb_2). The sphere defined by r_{ear} and the *n*s, *n*p$_z$, and *n*p$_y$ density surfaces for the N_2, P_2, As_2, and Sb_2 molecules are shown in Figures 2a-*i*, 2b-*i*, 2c-*i*, and 2d-*i* (i = 1, 2, 3), respectively.

Figure 2a-*i* shows that the sphere with radius r_{ear} for one of the N atoms covers completely the valence regions of another atom, according to the surface of density $|F(x,y,z)_{nl}|^2$. The two 2s spheres placed at $z = \pm R_e/2$ overlap slightly, the two

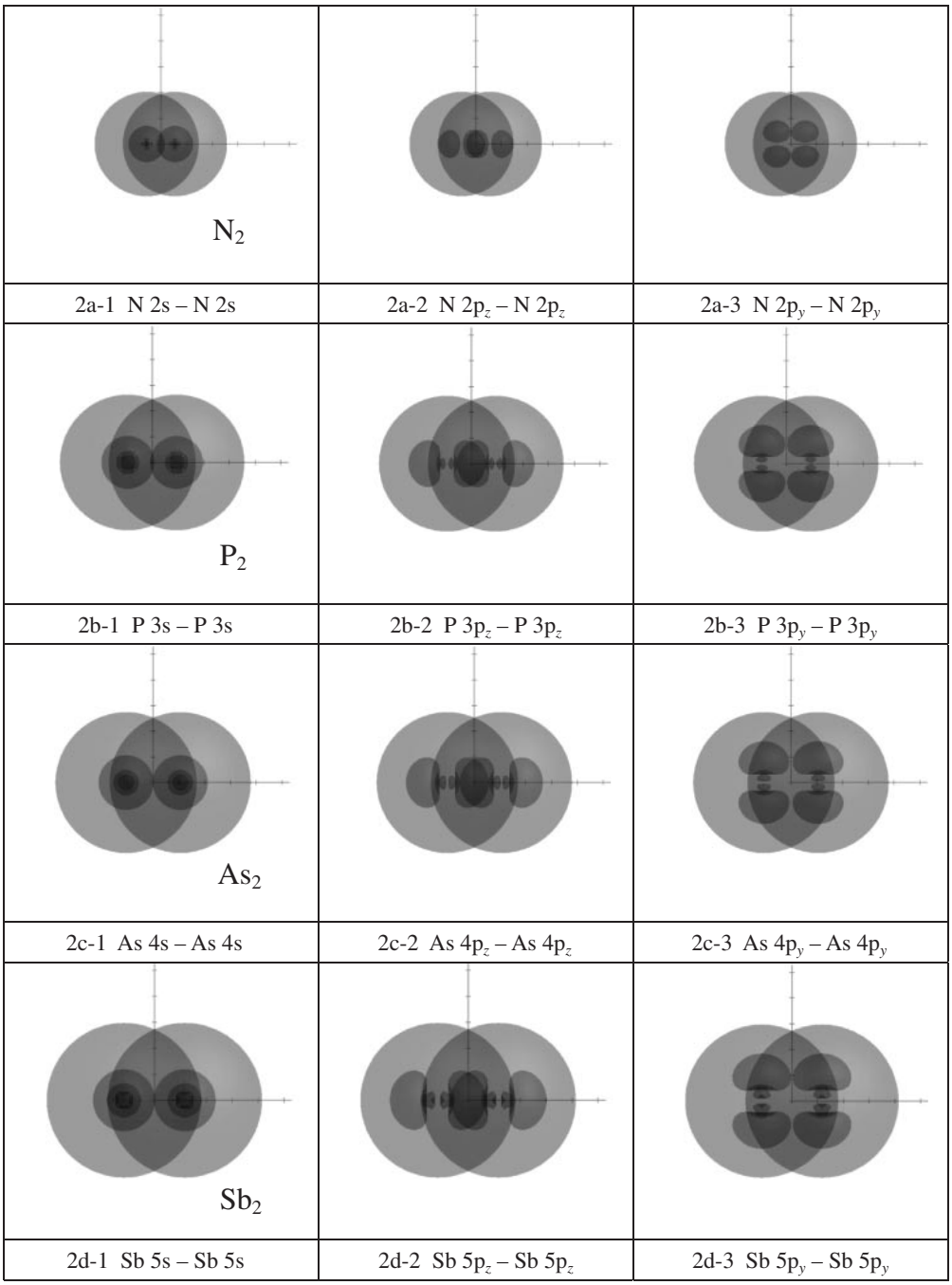

Figure 2. The sphere defined by r_{ear} and the ns, np$_z$, and np$_y$ density surfaces for diatomics of group 15: N_2, P_2, As_2, and Sb_2. (a) N_2, (b) P_2, (c) As_2, and (d) Sb_2.

2p$_z$ spatial regions overlap significantly, and the regions for 2p$_y$s/2p$_x$s contact each other, although the valence regions include only 57%–58% of the valence electrons. This reveals the origin of the multi-bond in N_2, and the reason why the equilibrium internuclear distance is small ($R_e = 1.098$ Å[17]) and the molecular dissociation is large ($D_e = 9.78$ eV[17]).

Using Figure 2b-*i*, let us discuss the P_2 molecule. The two valence 3s spheres contact, the two 3p$_z$ regions overlap to a large extent, and the two 3p$_y$s/3p$_x$s are slightly apart. The sphere with radius r_{ear} for one of the P atoms does not cover the valence regions of the other atom, even in 3p$_z$s. The discussion above indicates that the bonding is weaker in P_2 than in N_2. In fact, R_e (1.89 Å[17]) is larger and D_e (5.03 eV[17]) is smaller than the corresponding values for N_2 ($R_e = 1.098$ Å and $D_e = 9.78$ eV).

The smaller spatial overlap between the r_{ear} sphere and the valence regions in As_2 than in P_2 parallels the decreases in P_2 relative to N_2. In the case of As_2, similar decreases exist in the spatial overlaps between the valence regions. The bonding in As_2 should therefore be weaker than in P_2; it has larger R_e (2.10 Å[17]) and smaller D_e (3.96 eV[17]) than P_2 ($R_e = 1.89$ Å) and ($D_e = 5.03$ eV). Upon comparing the sphere of radius r_{ear} and

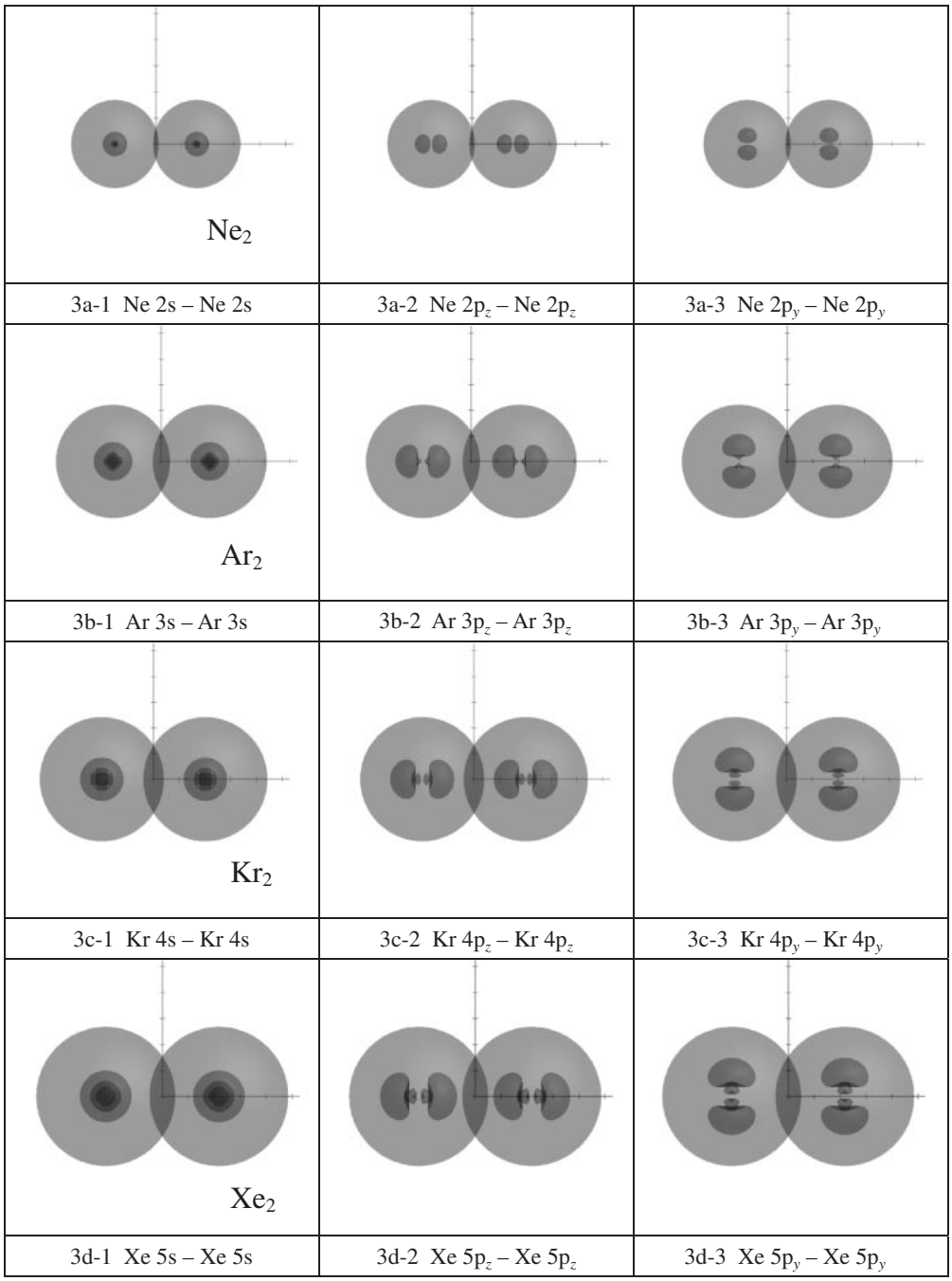

Figure 3. The sphere defined by r_{ear} and the ns, np$_z$, and np$_y$ density surfaces for diatomics of group 18: Ne_2, Ar_2, Kr_2, and Xe_2. (a) Ne_2, (b) Ar_2, (c) Kr_2, and (d) Xe_2.

the valence surfaces for Sb_2 with those of others, we understand why for Sb_2 D_e (3.09 eV[17]) is the smallest and R_e (2.34 Å[17]) is the largest of these diatomic molecules.

As discussed above, the internuclear distance is fixed to R_e. Under R_e such as in the group 15 diatomics, the density surfaces largely overlap or touch each other, indicating the electrostatic attraction of the ion core of the counter atom is strong. The new orbitals (molecular orbitals) are to be formed for describing the combined system appropriately. In the combined systems (diatomics) the main source of the molecular binding is the electrostatic attraction of the ion core of another atom which decreases as the atomic number increases, which is expected from Figure 2. The secondary source is the molecular extra electron correlations.

Group 18 Diatoms (Ne_2, Ar_2, Kr_2, and Xe_2). The sphere defined by r_{ear} and the ns, np$_z$, and np$_y$ density surfaces for the Ne_2, Ar_2, Kr_2, and Xe_2 molecules are shown in Figures 3a-*i*, 3b-*i*, 3c-*i*, and 3d-*i* ($i = 1, 2, 3$), respectively.

For Ne_2, the spheres with r_{ear} overlap slightly, while the two valence regions expressed by $|F(x,y,z)_{2p}|^2$ are far apart (Figure 3a-*i*), justifying the small D_e (0.002 eV[17]) and large R_e (3.15 Å[17]).

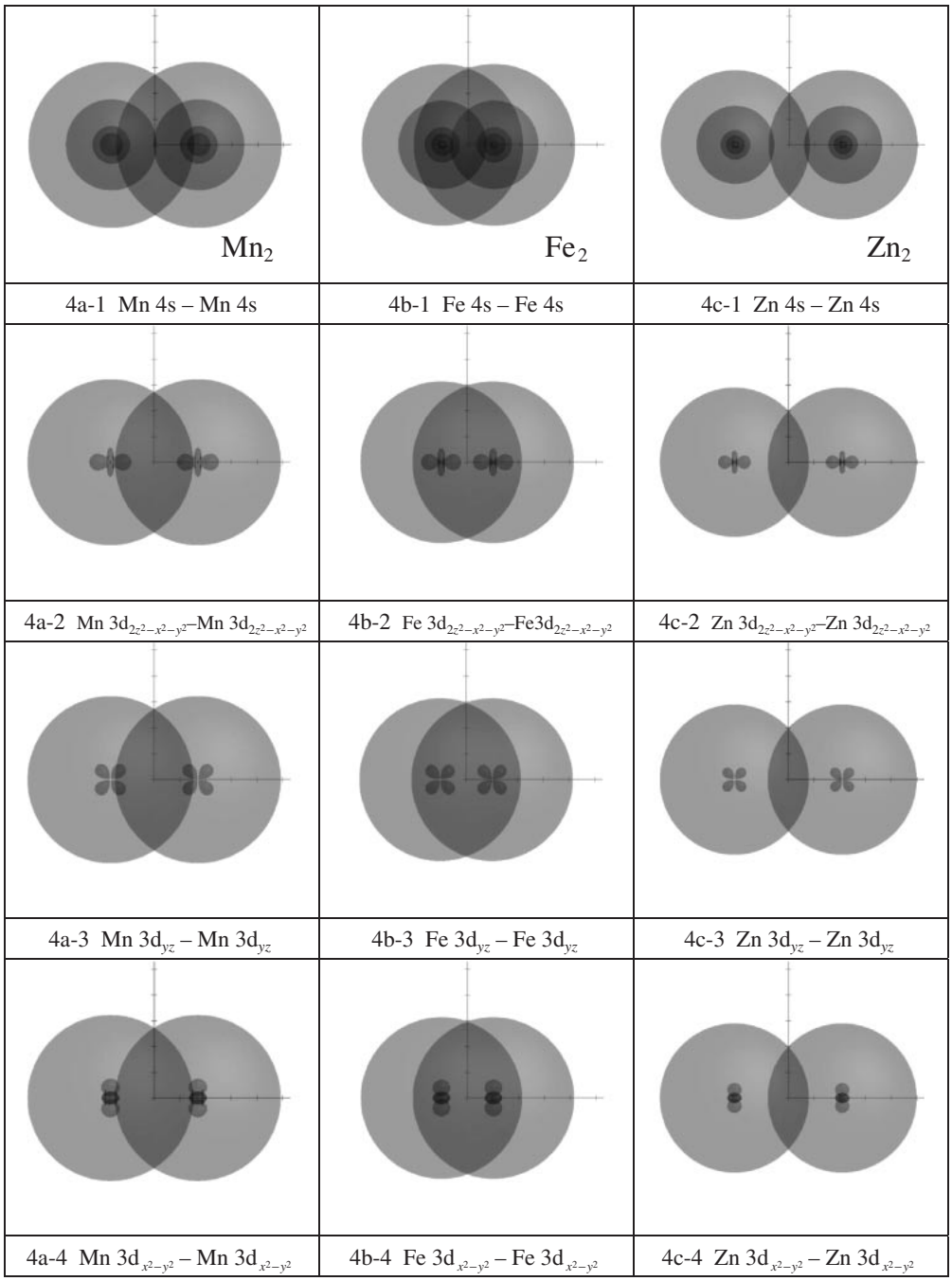

Figure 4. The sphere defined by r_{ear} and the 4s, $3d_{2z^2-x^2-y^2}$, $3d_{yz}$, and $3d_{x^2-y^2}$ density surfaces for transition-metal diatomics: Mn_2, Fe_2, and Zn_2. (a) Mn_2, (b) Fe_2, and (c) Zn_2.

In contrast to Ne_2, the overlap between spheres with radius r_{ear} increases for Ar_2 over that for Ne_2. We expect larger D_e (0.011 eV[17]) for Ar_2 than for Ne_2 (0.002 eV). The value of R_e (3.76 Å[17]) for Ar_2 is greater than that for Ne_2 (3.15 Å), reflecting the greater r_{ear} (2.21 Å) for Ar than for Ne (1.68 Å).

The overlap of spheres with radius r_{ear} is greater in Kr_2. We expect larger D_e (0.016 eV[17]) for Kr_2 than for Ar_2 (0.011 eV). The greater R_e (4.03 Å[17]) for Kr_2 than for Ar_2 (3.76 Å) reflects the greater r_{ear} (2.41 Å) of Kr than of Ar (2.21 Å). Comparison of the figures for Xe_2 with the others shows why the D_e value (0.023 eV[17]) of Xe_2 is the greatest among the inert gas diatomics. The R_e value for Xe_2 is 4.361 Å.[17]

As discussed above R_es for the group 18 diatomics are large enough to make the valence surfaces of the two atoms far apart. The electrostatic potential produced by the counter atom is small and the molecule is expected to be formed almost from the dynamical electron correlations including the dipole–dipole interactions.

Transition-Metal Diatoms (Mn_2, Fe_2, and Zn_2). Spectroscopic data for transition-metal diatomic molecules are scarce. We do not therefore consider the homonuclear diatomics belonging to the same group. We choose the three molecules Mn_2, Fe_2, and Zn_2, having the characteristics of the metallic, covalent (multiple), and van der Waals bondings respectively.

The sphere with radius r_{ear} and the 4s, $3d_{2z^2-x^2-y^2}$, $3d_{yz}$, and $3d_{x^2-y^2}$ density surfaces for Mn_2, Fe_2, and Zn_2 are shown in Figures 4a-*i*, 4b-*i*, and 4c-*i* ($i = 1$, 2, 3, 4), respectively. The 3s and 3p orbitals are valence orbitals, like 3d, but they are somewhat contracted relative to 3d and we have not shown their figures to save the space.

In Mn_2, spheres with radius $\langle r\rangle_{4s}$ touch each other, suggesting the large contribution of 4s electrons to the chemical bonding. The 3d surfaces belonging to the respective atoms are far apart. These 3d surfaces contain only 59% of the 3d electrons (Table 6). One may claim that the surface defined by these electron numbers is too small as giving the valence 3d region. We therefore drew the surfaces including 90% of 3d electrons similar to Figure 4a, and we found that they are again apart. We see also in Figure 4a-*i* that the sphere with radius r_{ear} overlaps with the spatial region spanned by the 3d orbitals (and also 3p and 3s) of the counter Mn atom, indicating the importance of the 4s electron interaction with 3d, 3p, and 3s electrons of the counter Mn atom. The experimental R_e value is 3.4 Å,[18] nearly twice $\langle r\rangle_{4s}$, is shorter than that of Kr_2 ($R_e = 4.03$ Å) and D_e is 0.1 eV[18] which is 6 times greater than that of Kr_2. Since 1) the spheres with $\langle r\rangle_{4s}$ touch with each other, 2) the two 4s orbitals considerably overlap, and 3) the 4s interaction with 3d, 3p, and 3s electrons of another Mn is important, the van der Waals bonding is not suitable for characterizing Mn_2. The metallic bonding is preferable where the 4s electrons move in the field generated by the ion core formed with a nucleus and electrons in the 3d, 3p, and 3s orbitals as in the Mn solid.

In Fe_2, the two spheres with radius $\langle r\rangle_{4s}$ overlap greatly, as shown in Figure 4b-1. This sphere encloses the valence regions of 3ds of the counter Fe atom. The two valence regions covered by the $3d_{2z^2-x^2-y^2}$ surface are close to each other. We therefore expect that Fe_2 has multibond character, having smaller R_e (2.02 A[19]) and larger D_e (1.30 ± 0.20 eV[20]) than Mn_2 ($R_e = 3.4$ Å and $D_e = 0.1$ eV).

Finally, we discuss Zn_2. Figure 4c shows that the spheres with radius r_{ear} overlap, but the regions enclosed by the 4s and 3d surfaces including NVE given in Table 5 are as far apart as in the inert gas diatomics, suggesting that Zn_2 is a van der Waals molecule. The experimental R_e and D_e values are respectively longer (4.19 Å[21]) and larger (0.035 eV[21]) than those of Kr_2 ($R_e = 4.03$ Å and $D_e = 0.016$ eV).

Summary

We have developed the effective atomic radius r_{ear} at which the magnitude of the electric field is that in He at one half of the equilibrium bond length of He_2; $r_{ear} = r$ at which $E = E_{He}$ ($r = R_e/2$ of He_2) This radius correctly reflects the electronic configuration of the atomic ground state. In summary, r_{ear} decreases as the atomic number increases for typical atoms having the configuration ns^2np^m. For the second transition metal atoms, we have three nearly degenerate configurations: $5s^24d^m$, $5s^14d^{m+1}$, and $5s^04d^{m+2}$. There are therefore three categories of r_{ear}, namely $r_{ear}(5s^24d^m)$, $r_{ear}(5s^14d^{m+1})$, and $r_{ear}(5s^04d^{m+2})$. The r_{ear} is uniquely determined to be one of the three, according to the optimum configuration. Similar results are found in the first transition metal atoms. In contrast, the experimental van der Waals radii or Bondi radii exhibit somewhat arbitrary behavior as the atomic number increases. Sometimes they are too small to specify the distance at which the interatomic interaction begins. The valence radius r_{val}, which was defined by $\langle r\rangle_i$ where i expresses the valence orbitals, has also been examined. Based on the values of r_{ear} and r_{val}, we have discussed the characteristics of the homonuclear diatomic molecules. The spheres of radius r_{ear} and r_{val} provide insight into why the multibonding in the group 15 diatomic molecules weakens from N_2 to Sb_2, and why the van der Waals interaction in group 18 increases from Ne_2 to Xe_2. These radii also explain the differences in the bonding of the transition diatomics Mn_2, Fe_2, and Zn_2, either metallic, multi (covalent), or van der Waals. In conclusion, we have successfully identified atomic radii suitable for depicting the extent of the charge distribution of atoms in a molecular skeleton.

References

1 T. Naka, Y. Hatano, S. Yamamoto, T. Noro, H. Tatewaki, *Bull. Chem. Soc. Jpn.* **2010**, *83*, 782.

2 L. Pauling, *The Nature of the Chemical Bond*, 3rd ed., Cornell University Press, Ithaca, New York, **1960**.

3 W. L. Bragg, *Philos. Mag. Ser. 6* **1920**, *40*, 169.

4 J. C. Slater, *J. Chem. Phys.* **1964**, *41*, 3199.

5 Z.-Z. Yang, E. R. Davidson, *Int. J. Quantum Chem.* **1997**, *62*, 47.

6 A. Bondi, *J. Phys. Chem.* **1964**, *68*, 441.

7 M. Mantina, A. C. Chamberlin, R. Valeo, C. J. Cramer, D. G. Truhlar, *J. Phys. Chem. A* **2009**, *113*, 5806.

8 M. Douglas, N. M. Kroll, *Ann. Phys.* **1974**, *82*, 89.

9 B. A. Hess, *Phys. Rev. A* **1986**, *33*, 3742.

10 *GAMESS*, version 10, November, **2004**; M. W. Schmidt, K. K. Baldridge, J. A. Boatz, S. T. Elbert, M. S. Gordon, J. H. Jensen, S. Koseki, N. Matsunaga, K. A. Nguyen, S. Su, T. L. Windus, M. Dupuis, J. A. Montgomery, Jr., *J. Comput. Chem.* **1993**, *14*, 1347.

11 T. Nakajima, K. Hirao, *Chem. Phys. Lett.* **2000**, *329*, 511.

12 T. Noro, M. Sekiya, T. Koga, *Chem. Phys. Lett.*, to be submitted.

13 V. Kellö, A. J. Sadlej, B. A. Hess, *J. Chem. Phys.* **1996**, *105*, 1995.

14 V. Kellö, A. J. Sadlej, *Int. J. Quantum Chem.* **1998**, *68*, 159.

15 R. Mastalerz, G. Barone, R. Lindh, M. Reiher, *J. Chem. Phys.* **2007**, *127*, 074105.

16 J. Seino, W. Uesugi, M. Hada, *J. Chem. Phys.* **2010**, *132*, 164108.

17 K. P. Hubner, G. Herzberg, *Molecular Spectra and Molecular Structure IV. Constants of Diatomic Molecules*, Van Nostrand Reinhold, New York, **1978**.

18 A. D. Kirkwood, K. D. Bier, J. K. Thompson, T. L. Haslett, A. S. Huber, M. Moskovits, *J. Phys. Chem.* **1991**, *95*, 2644.

19 H. Purdum, P. A. Montano, G. K. Shenoy, T. Morrison, *Phys. Rev.* **1982**, *B25*, 4412.

20 M. Moskovits, D. P. DiLella, W. Limm, *J. Chem. Phys.* **1984**, *80*, 626.

21 M. A. Czajkowski, J. Koperski, *Spectrochim. Acta, Part A* **1999**, *55*, 2221.